Neutrino Oscillations and Non-standard Interactions with KM3NeT-ORCA

N. R. Khan Chowdhury on behalf of the KM3NeT Collaboration

IFIC - Instituto de Fisica Corpuscular (Univ. de Valencia - CSIC)

nafis.chowdhury@ific.uv.es

Abstract

ORCA (Oscillations Research with Cosmics in the Abyss) is the low-energy node of KM3NeT, the next generation underwater Cherenkov neutrino detector in the Mediterranean sea. The primary goal of KM3NeT-ORCA is the determination of the neutrino mass ordering (NMO). With an energy threshold of few GeV and an effective mass of several Mtons, KM3NeT-ORCA can also make precision measurements of atmospheric oscillation parameters. Moreover, its access to a wide range of energies and baselines makes it optimal to discover exotic physics beyond the Standard Model such as Non-Standard Interactions (NSI) of neutrinos. The sensitivity of the detector to the neutrino mass ordering is presented, along with its potential for determination of the atmospheric oscillation parameters. It is observed that KM3NeT-ORCA will improve the current upper limits on NSI parameters by an order of magnitude after three years of data taking.

Presented at

NuPhys2019: Prospects in Neutrino Physics
Cavendish Conference Centre, London, 16–18 December 2019

1 Introduction

The conventional model of neutrino oscillations provides a successful interpretation of data taken by various solar [1], atmospheric [2], accelerator [3] and reactor [4–6] experiments. Crucial goals of future oscillation experiments can be grouped as (a) the determination of the neutrino mass ordering and the CP-violating phase δ with precise measurement of oscillation parameters, and (b) establishing the robustness of the standard three-flavor oscillation hypothesis with respect to physics beyond the Standard Model. In the present work we show the physics potential of KM3NeT-ORCA [7] in trying to pin down these open questions.

The matter-induced modifications of neutrino oscillation probabilities is different for neutrino and anti-neutrino channels and is a function of neutrino mass ordering. In Fig. 1, if we consider the $P_{e\mu}$ and $P_{\bar{e}\bar{\mu}}$ appearance channels, one sees an enhancement in $P_{e\mu}$ and suppression in $P_{\bar{e}\bar{\mu}}$ if ordering is normal (NO) while if the ordering is inverted (IO), one gets the reverse. These ordering dependent alterations of oscillation signals discernible at few GeV give a handle to disentangle the two mass orderings.
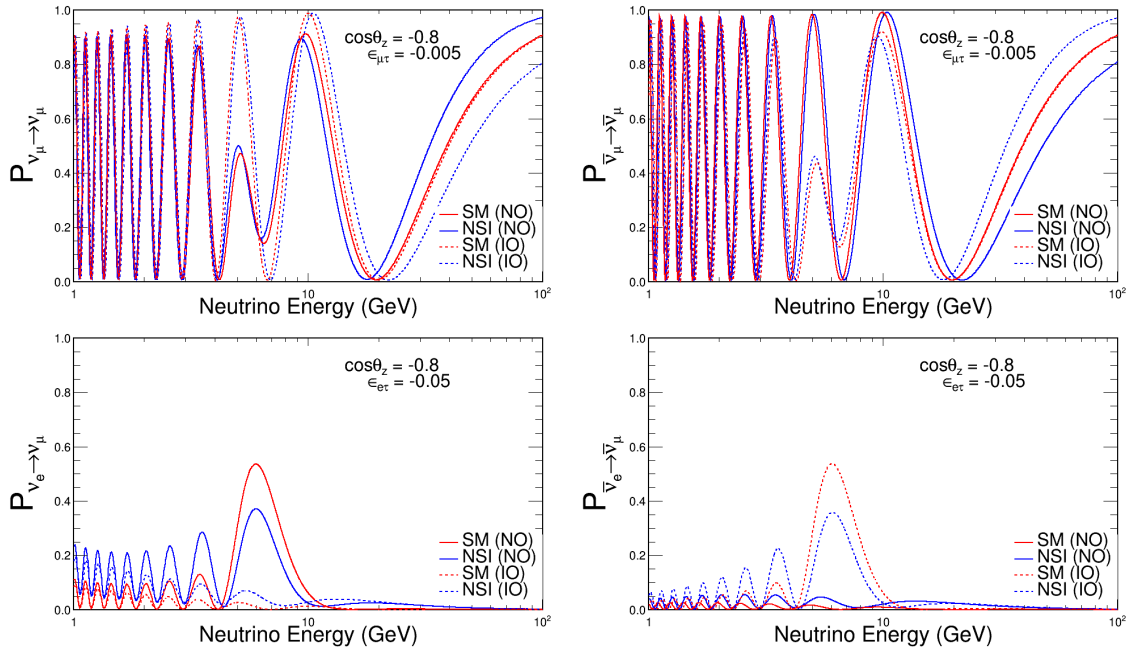

Figure 1: Oscillation probabilities in the $\nu_\mu \to \nu_\mu$ (top) and $\nu_e \to \nu_\mu$ (bottom) channel as a function of neutrino energy for a fixed value of zenith angle (θ_z). The solid (dashed) curves are for NO (IO). (Anti-)Neutrinos on the (right) left. The values of NSI parameters for which the blue curves are drawn are quoted.

In addition to the Standard Model (SM) MSW resonance, flavour changing neutral current (NC) Non-Standard Interactions (NSI) [8,9] of neutrinos (of all flavours) with fermions (e, u and d-quarks) present in Earth would alter the oscillation probabilities. NSI of neutrinos in propagation can be modelled as perturbations in the standard neutrino propagation Hamiltonian as,

$$H = \frac{1}{2E}U\begin{bmatrix} 0 & 0 & 0 \\ 0 & \Delta m_{21}^2 & 0 \\ 0 & 0 & \Delta m_{31}^2 \end{bmatrix}U^\dagger + 2\sqrt{2}G_F N_f(x)\begin{bmatrix} 1+\epsilon_{ee} & \epsilon_{e\mu} & \epsilon_{e\tau} \\ \epsilon_{e\mu}^* & \epsilon_{\mu\mu} & \epsilon_{\mu\tau} \\ \epsilon_{e\tau}^* & \epsilon_{\mu\tau}^* & \epsilon_{\tau\tau} \end{bmatrix}. \quad (1)$$

2

G_F is the Fermi coupling constant, $N_f(x)$ is the fermion number density along the neutrino path, and the $\epsilon_{\alpha\beta}$ represent the NSI coupling parameters. In this analysis, we consider non-standard interactions between neutrinos and d-quarks present in the Earth. The effect of the presence of non-standard interactions at one of the most dominant channels at ORCA is shown is Fig. 1. The effect for neutrinos in the Normal Ordering (NO) is similar to anti-neutrinos in the Inverted Ordering (IO) .

2   The KM3NeT-ORCA detector

The KM3NeT-ORCA detector [7], currently being installed at a depth of 2450 m in the Mediterranean Sea, is a megaton-scale water Cherenkov detector located 40 km offshore Toulon, France. Upon completion, the detector will consist of 115 detection units (DUs), each of which will comprise 18 spherical, 17" diameter Digital Optical Modules (DOMs) housing 31 3" PMTs and associated electronics. The average vertical spacing between the DOMs is 9 m and the horizontal spacing between the DUs is 23 m, amounting to a total instrumented volume of $\sim$8 Mton. The granularity of the detector layout makes it optimal to detect neutrinos with energies as low as $\sim$3 GeV.
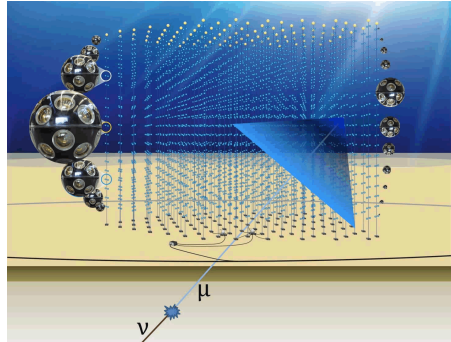

Figure 2: An artist's impression of the detector is shown.

3   Event spectra at the detector

The HKKM 2014 [10] flux tables (Gran Sasso site) are interpolated in $\log_{10}(E)$ and $\cos\theta_z$ and multiplied with the detector effective mass to calculate the rate of events for each interaction channel: ν_x charged current (CC), $\bar{\nu}_x$ CC (x = e, μ, τ), ν neutral current (NC) and $\bar{\nu}$ NC. Depending on the Cherenkov signatures of the outgoing lepton, two distinct event topologies are observed at the detector: track-like (left) and shower-like events (right). While ν_μ CC interactions mostly account for track-like topology, shower-like topology has events from both ν_e CC and NC interactions.

The statistical χ^2 for each (E, θ_z) bin is computed from,

$$\chi^2_{\mathrm{E},\theta_z}(\epsilon_{\alpha\beta}) = \frac{\left(N^{\mathrm{model}}_{\mathrm{E},\theta_z}(\epsilon_{\alpha\beta}) - N^{\mathrm{data}}_{\mathrm{E},\theta_z}(\epsilon_{\alpha\beta}=0)\right) \times \left|N^{\mathrm{model}}_{\mathrm{E},\theta_z}(\epsilon_{\alpha\beta}) - N^{\mathrm{data}}_{\mathrm{E},\theta_z}(\epsilon_{\alpha\beta}=0)\right|}{N^{\mathrm{data}}_{\mathrm{E},\theta_z}(\epsilon_{\alpha\beta}=0)}, \quad (2)$$

where the superscript model represents the NSI case with $\epsilon_{e\tau} = -0.05$. All other NSI parameters are fixed at zero. Figure 4 shows the signed-χ^2 maps for reconstructed events in the track-like and shower-like event topologies for three years of full KM3NeT-ORCA (115 DUs) runtime. 20 logarithmic bins were chosen in reconstructed neutrino energy (E) between 3 and 100 GeV, and 20 linear bins in cosine of the reconstructed zenith angle (θ_z) between -1 and 0.
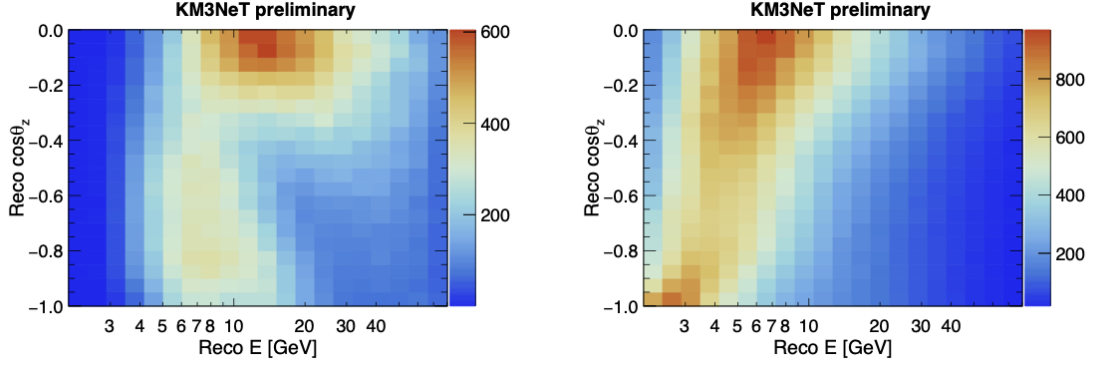
Figure 3: Two distinct event topologies at ORCA: tracks (left) and showers (right). Oscillation parameters are adopted from NuFit 3.2 [11] with NO assumption.
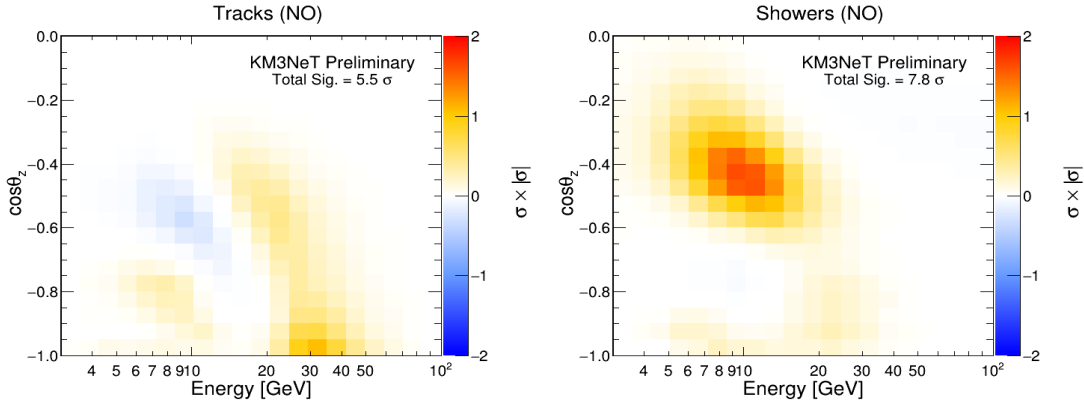

Figure 4: Statistical χ^2 as a function of reconstructed neutrino energy (E) and direction ($\cos\theta_z$) for track-like (left) and shower-like (right) event topologies. NO is assumed. The colour code indicates the excess and deficits of events from the SM predictions. The total sensitivity quoted is the sum of the absolute value of the statistical χ^2 for each bin.

4 Systematics

The final sensitivities of the experiment to NMO (or NSI) is estimated with a log-likelihood ratio test statistic based on the Asimov approach [12]:

$$
\chi^2_{\text{NMO/NSI}} = 2 \sum_{E,\theta_z} \left(N^{\text{WO/NSI}}_{E,\theta_z}(\epsilon_{\alpha\beta}) \left(1 + \sum_k f^k_{E,\theta_z} \zeta_k \right) - N^{\text{RO/SM}}_{E,\theta_z}(\epsilon_{\alpha\beta} = 0) \right.
$$
$$
\left. + N^{\text{RO/SM}}_{E,\theta_z}(\epsilon_{\alpha\beta} = 0) \ln \frac{N^{\text{RO/SM}}_{E,\theta_z}(\epsilon_{\alpha\beta} = 0)}{N^{\text{WO/NSI}}_{E,\theta_z}(\epsilon_{\alpha\beta}) \left(1 + \sum_k f^k_{E,\theta_z} \zeta_k \right)} \right) + \sum_k \zeta_k^2. \quad (3)
$$

$N^{\text{RO}}_{E,\theta_z}$ ($N^{\text{WO}}_{E,\theta_z}$) denotes the expected number of track / shower events in a given $[E, \theta_z]$ bin for the right ordering (wrong ordering) hypothesis in the standard 3ν oscillation framework. In the case of NSI sensitivity estimation, $N^{\text{NSI}}_{E,\theta_z}$ ($N^{\text{SM}}_{E,\theta_z}$) is the predicted number of events for an assumed mass ordering in presence (absence) of NSI.

Systematics are included in our simulation using the "pull" method [12, 13]. Table 1 lists nuisance parameters and oscillation parameters adopted from NuFit 3.2 [11] and their corresponding Gaussian priors (if any) over which marginalisation has been done to minimise the value of $\chi^2_{\text{NMO/NSI}}$. The individual contributions from track-like and shower-like events are added in quadrature to compute the total significance.

Table 1: List of systematics.

parameters	treatment	true values	prior
$\Delta m^2_{21}/10^{-5}eV^2$	fix	7.40	-
$\Delta m^2_{31}/10^{-3}eV^2$	fitted	2.494	free
$\theta_{12}(°)$	fix	33.62	-
$\theta_{13}(°)$	fitted	8.54	0.15
$\theta_{23}(°)$	fitted	47.2	free
$\delta_{CP}(°)$	fitted	234	free
Flux norm.	fitted	1	10%
NC scale	fitted	1	5%
Energy slope	fitted	1	3%
ν_μ/ν_e skew	fitted	0	5%
$\nu/\bar{\nu}$ skew	fitted	0	3%

5 Results

5.1 Neutrino Oscillations

The Asimov NMO sensitivity [14] for three years of KM3NeT-ORCA runtime is shown in Fig. 5 (left) for a range of possible true θ_{23} values . The curves are drawn for both assumed true orderings and the most favourable and least favourable δ_{CP} values.
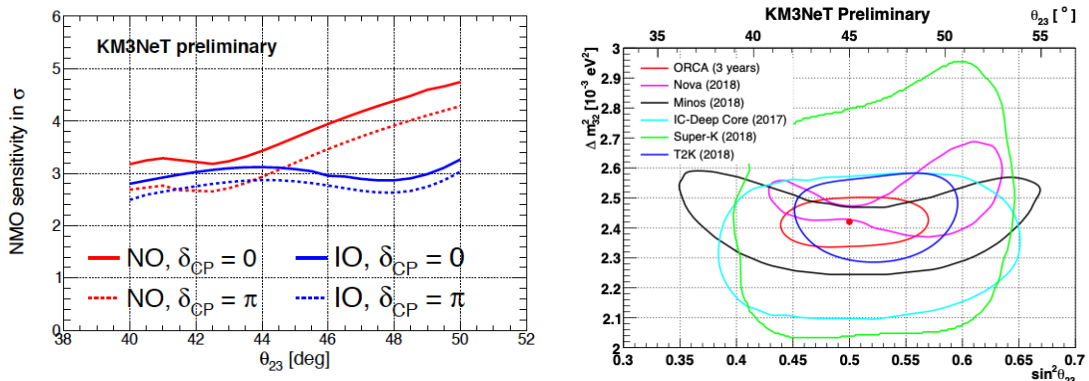

Figure 5: Projected sensitivity to NMO (left) for truth NO (red) and IO (blue) assumptions. Exclusion plot in θ_{23} - Δm^2_{32} plane on the right .

Allowed region of atmospheric oscillation parameters by KM3NeT-ORCA [14] after three years of running is shown in Fig. 5 (right), overlapped with current constraints from MINOS [15], NOνA [16], Super-K [17] and IceCube-DeepCore [18]. The 90% CL contour is drawn assuming NO (fixed) and $\delta_{CP} = 0$ (fitted).

5.2 Non-standard Interactions

The 90% C.L. contours in correlated NSI parameter spaces allowed after three years of data taking of KM3NeT-ORCA are shown for both orderings assumptions. The NSI parameters not appearing on the plots are fixed at zero.
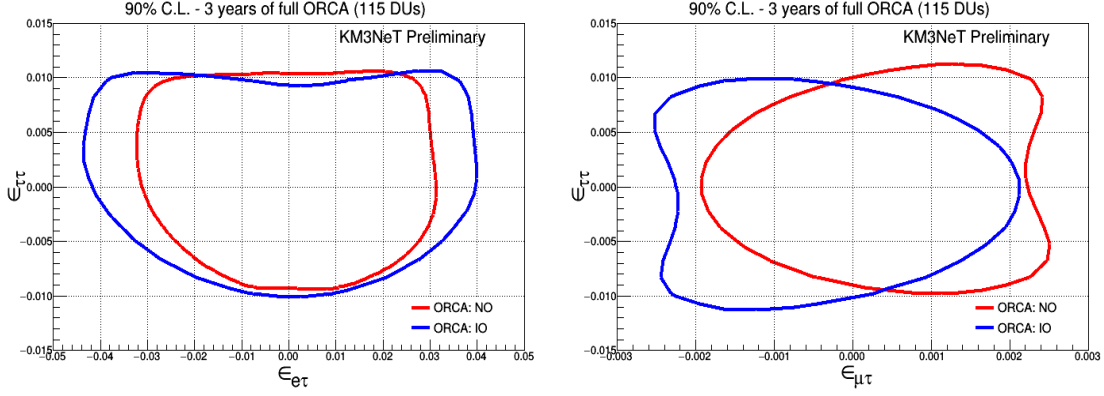
Figure 6: Allowed region in correlated NSI parameter phase spaces $|\epsilon_{e\tau} - \epsilon_{\tau\tau}|$ (left) and $|\epsilon_{\mu\tau} - \epsilon_{\tau\tau}|$ (right) after three years of ORCA runtime. Pseudo data is generated for $(\epsilon_{ij}, \epsilon_{kl}) = (0, 0)$.
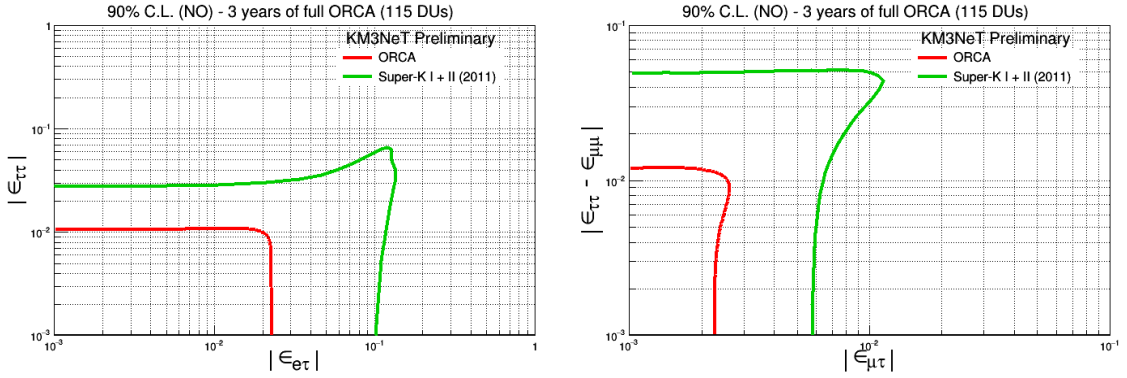

Figure 7: Allowed NSI parameter regions in the $e - \tau$ sector (left) for $\epsilon_{ee} = 0$ and $\mu - \tau$ sector (right) in the *hybrid model* approximation [19] are shown.
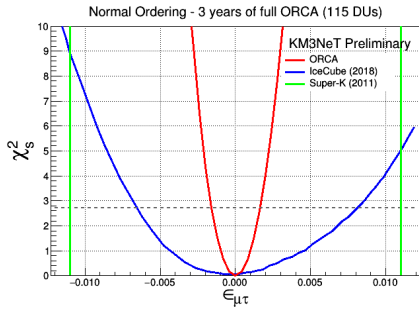

Figure 8: Sensitivity to $\epsilon_{\mu\tau}$.

In Figure 7 and 8, the exclusion region assuming NO in the *hybrid model* approximation (θ_{12}, θ_{13}, and $\Delta m_{21}^2 = 0$) is drawn for comparison with IceCube [20] and Super-K [19]. With three years of run time, ORCA is expected to constrain NSI parameters $\epsilon_{e\tau}$, $\epsilon_{\mu\tau}$ and $\epsilon_{\tau\tau}$ by a factor of four better than current limits.

6 Summary

In this contribution, future projections of sensitivity of KM3NeT-ORCA towards neutrino mass ordering resolution and precise measurement of atmospheric oscillation parameters has been reported. The impact of non-standard interactions on the event signal at KM3NeT-ORCA is probed and its discovery potential to different NSI phase spaces has been discussed.

References

[1] Q. R. Ahmad et al. Direct evidence for neutrino flavor transformation from neutral current interactions in the Sudbury Neutrino Observatory. *Phys. Rev. Lett.*, 89:011301, 2002.

[2] Y. Fukuda et al. Evidence for oscillation of atmospheric neutrinos. *Phys. Rev. Lett.*, 81:1562–1567, 1998.

[3] K. Abe et al. Indication of Electron Neutrino Appearance from an Accelerator-produced Off-axis Muon Neutrino Beam. *Phys. Rev. Lett.*, 107:041801, 2011.

[4] K. Eguchi et al. First results from KamLAND: Evidence for reactor anti-neutrino disappearance. *Phys. Rev. Lett.*, 90:021802, 2003.

[5] Y. Abe et al. Indication of Reactor $\bar{\nu}_e$ Disappearance in the Double Chooz Experiment. *Phys. Rev. Lett.*, 108:131801, 2012.

[6] F. P. An et al. Observation of electron-antineutrino disappearance at Daya Bay. *Phys. Rev. Lett.*, 108:171803, 2012.

[7] S. Adrian-Martinez et al. Letter of intent for KM3NeT 2.0. *J. Phys.*, G43(8):084001, 2016.

[8] Tommy Ohlsson. Status of non-standard neutrino interactions. *Rept. Prog. Phys.*, 76:044201, 2013.

[9] Y. Farzan and M. Tortola. Neutrino oscillations and Non-Standard Interactions. *Front.in Phys.*, 6:10, 2018.

[10] M. Honda, M. Sajjad Athar, T. Kajita, K. Kasahara, and S. Midorikawa. Atmospheric neutrino flux calculation using the NRLMSISE-00 atmospheric model. *Phys. Rev.*, D92(2):023004, 2015.

[11] Ivan Esteban, M. C. Gonzalez-Garcia, Michele Maltoni, Ivan Martinez-Soler, and Thomas Schwetz. Updated fit to three neutrino mixing: exploring the accelerator-reactor complementarity. *JHEP*, 01:087, 2017.

[12] R. Gandhi, P. Ghoshal, S. Goswami, P. Mehta, S. U. Sankar, and S. Shalgar. Mass Hierarchy Determination via future Atmospheric Neutrino Detectors. *Phys. Rev.*, D76:073012, 2007.

[13] A. Ghosh, T. Thakore, and S. Choubey. Determining the Neutrino Mass Hierarchy with INO, T2K, NOvA and Reactor Experiments. *JHEP*, 04:009, 2013.

[14] Bruno Strandberg Steffen Hallmann. Neutrino oscillation research with KM3NeT/ORCA. $https://pos.sissa.it/358/1019/pdf$, 2019.

[15] Alec Habig. MINOS neutrino oscillation results. *Mod. Phys. Lett.*, A25:1219–1231, 2010.

[16] M. A. Acero et al. First Measurement of Neutrino Oscillation Parameters using Neutrinos and Antineutrinos by NOvA. *Phys. Rev. Lett.*, 123(15):151803, 2019.

[17] Y. Ashie et al. A Measurement of atmospheric neutrino oscillation parameters by SUPER-KAMIOKANDE I. *Phys. Rev.*, D71:112005, 2005.

[18] M. G. Aartsen et al. Measurement of Atmospheric Neutrino Oscillations at 6–56 GeV with IceCube DeepCore. *Phys. Rev. Lett.*, 120(7):071801, 2018.

[19] G. Mitsuka et al. Study of Non-Standard Neutrino Interactions with Atmospheric Neutrino Data in Super-Kamiokande I and II. *Phys. Rev.*, D84:113008, 2011.

[20] M. G. Aartsen et al. Search for Nonstandard Neutrino Interactions with IceCube DeepCore. *Phys. Rev.*, D97(7):072009, 2018.